



Published in final edited form as:

Pain. 2020 September 01; 161(9): 2107–2118. doi:10.1097/j.pain.0000000000001888.

Activation of sphingosine-1-phosphate receptor subtype 1 in the central nervous system contributes to morphine-induced hyperalgesia and antinociceptive tolerance in rodents

Timothy M. Doyle^{1,2}, Kali Janes¹, Zhoumou Chen^{1,2}, Peter M. Grace³, Emanuela Esposito⁴, Salvatore Cuzzocrea⁴, Tally M. Largent-Milnes⁵, William L. Neumann⁶, Linda R. Watkins⁷, Sarah Spiegel⁸, Todd W. Vanderah⁵, Daniela Salvemini^{1,2,§}

¹Department of Pharmacology and Physiology, Saint Louis University School of Medicine, 1402 South Grand Blvd, St. Louis, MO 63104, USA.

²Henry and Amelia Nasrallah Center for Neuroscience, Saint Louis University School of Medicine, 1402 South Grand Blvd, St. Louis, MO 63104, USA.

³Department of Symptom Research University of Texas MD Anderson Cancer Center, Houston, TX 77030, USA.

⁴Department of Clinical and Experimental Medicine and Pharmacology, University of Messina, Messina 98122 Italy.

⁵Department of Pharmacology, University of Arizona College of Medicine, Tucson, AZ 85724, USA

⁶Department of Pharmaceutical Sciences, School of Pharmacy, Southern Illinois University Edwardsville, 200 University Park, Edwardsville, IL 62026, USA.

⁷Department of Psychology and Neuroscience, University of Colorado, Boulder, CO 80309, USA.

⁸Department of Biochemistry and Molecular Biology, Virginia Commonwealth University; School of Medicine, 1101 E Marshall St, Richmond, VA 23298, USA.

Introduction

Treating chronic pain is difficult and often involves prescribing opioids. However, the long-term use of opioids, such as morphine, is limited by emergence of opioid-induced hyperalgesia (OIH), a sensitization process where opioids cause paradoxical development of painful hypersensitivity, and antinociceptive tolerance, a reduction in antinociceptive response to opioids over time [2; 12]. These adverse opioid-induced effects contribute to the loss of antinociceptive effectiveness of opioids that often prompts extended use and escalated dosages that over time can lead to additional unwanted side effects such as

[§]Corresponding author: daniela.salvemini@health.slu.edu, Phone: 1-314-977-6430, Fax: 1-314-977-6441, Address: 1402 South Grand Blvd, St. Louis, MO 63104, USA.

Author contributions: Performed experiments and analyzed data: TMD, KJ, ZC, EE, SC, TML and PMG. Synthesized compounds: WLM. Designed experiments: LRW. Assisted in writing manuscript: TD, PMG, TML, WLM and SS. Conceived experiments, directed the studies and wrote the manuscript: TWV and DS.

Disclosure: All other authors declare no conflict of interest.

dependence, addiction and abuse [2; 12]. Despite the serious side effects hindering long-term opioid use, there remains a strong reliance on this class of drugs for pain management [73]. Accordingly, continued investigation of the molecular underpinnings is essential for identifying opioid-sparing approaches.

We have previously reported that sustained morphine exposure in rodents caused the dysregulation of sphingolipid metabolism in the dorsal horn of the spinal cord evident by significantly increased production of the pro-inflammatory, pro-apoptotic ceramide and its downstream pro-inflammatory, anti-apoptotic bioactive sphingolipid metabolite, sphingosine-1-phosphate (S1P) [53]. S1P is produced through ceramidase conversion of ceramide to sphingosine and subsequent phosphorylation by sphingosine kinases 1 or 2 [38; 45]. All cells possess the enzymatic machinery to synthesize and metabolize S1P [43; 56]. Our previous work also revealed that reducing ceramide and S1P formation in the spinal cord through inhibition of sphingolipid metabolic enzymes or sphingosine kinases blocked the development of OIH and antinociceptive tolerance [53]. Many of the biological actions of S1P are mediated by five G protein-coupled receptors (S1PR1–5) [64] and analyses of their distribution under normal and disease varies among the cells of the central nervous system (CNS): astrocytes and microglia (S1PR1, S1PR3 and some S1PR2 and 5), neurons (S1PR1, S1PR2, S1PR3) and oligodendrocytes (S1PR5 and small amounts of S1PR1) [10; 28; 31; 71; 79]. S1PR4 is largely restricted to immune cells [10; 28]. However, S1P also exerts its effect through intracellular targets [38; 45]. How S1P exerts its effects in response to opioids is not known. Filling these gaps is critical in fostering our understanding of sphingolipid and opioid interactions and research efforts towards the identification of novel therapeutic approaches. Here, we provide the first evidence that activation of spinal S1PR1 contributes to the development of OIH and antinociceptive tolerance.

Materials and methods

Study approval.

All animal studies were performed in accordance with the International Association for the Study of Pain, the National Institutes of Health guidelines on laboratory animal welfare, regulations in Italy (DM 116192) and EU (OJ of EC L 358/112/18/1986) and approved by the Saint Louis University Institutional Animal Care and Use Committee, University of Arizona Animal Care and Use Committee, the University of Messina Review Board for the care of animals and the Institutional Animal Care and Use Committee of the University of Colorado Boulder.

Animal.

Pathogen-free adult male and female Sprague Dawley rats (200–225g) from Harlan Laboratories (Nossan, Milan, Italy and Indianapolis IN, USA; Frederik MD, USA breeding colony) or Fischer 344 (F344) rats (12 weeks old on arrival; Harlan Labs, Indianapolis, IN) were housed 3–4 per cage. Adult male CD-1 mice (20–30g; Harlan Laboratories) were housed 4–5 per cage. All animals were kept in a controlled environment (12h light/dark cycle) with food and water available *ad libitum*. Animals were randomly segregated into treatment groups for each experiment and the experimenters were blinded to the sex and

treatment during behavior and biochemical assessments. Animals were excluded when exhibiting adverse health effects not related to OIH, tolerance or neuropathic pain, such as piloerection, motor insufficiency, periorbital bleeding, lethargy.

Test compounds.

Morphine sulfate used in most studies was a kind gift from Mallinckrodt Pharmaceuticals (St. Louis MO, USA) or obtained from the NIDA drug depository (Bethesda MD, USA) for withdrawal studies. Fingolimod (FTY720; Gilenya®), W146, W140, JTE-013, CAY10444, and SEW2871 were purchased from Cayman Chemical (Ann Arbor, MI). Ponesimod [5] was synthesized by Shanghai ChemPartner Co (purity of >95%; Shanghai, China). The Novartis competitive antagonist (S)-2-([3'-(4-chloro-2,5-dimethylphenylsulfonylamino)-3,5-dimethylbiphenyl-4-carbonylmethylamino]-4-dimethylaminobutyric acid methyl ester 14 (NIBR-14; MW= 600.17) and NIBR-15 (purity of >95%) were prepared as described in the literature [1].

Intrathecal and systemic delivery of test agents.

All agents or their vehicle (1–5% DMSO in saline) were given by intrathecal injection (10 µl) through chronic intrathecal cannulas implanted as previously described [70]. Following the injection, the catheter was flushed with sterile physiological saline (12 µl). Animals were singly housed following surgery and allowed to recover for 7 days. Test substances or their vehicle given by systemic administration were delivered in a 0.2 ml dosing volume. DMSO (2–5%) was used as a vehicle for intraperitoneal injections and 10% DMSO/5% methylcellulose was for oral administration.

Silencing spinal *S1pr1* with siRNA.

Commercially available 27mer duplex dicer substrate siRNA (DsiRNA) targeting common splice-forms of *S1pr1*/Edg1 transcript (Accession number: NM_017301; Integrated DNA Technologies, Coralville, IA; #RNC.RNAL.N017301.12.1; 5'-rCrCrUrGrUrArCrArArArGrCrArGrArGrUrArCrUrUrCrCT G-3', 5'-rCrArGrGrArArGrUrArCrUrCrUrGrCrUrUrGrUrArCrArGrGrArU-3') or its non-targeting control sequence (siNT; Integrated DNA Technologies, Coralville, IA; #DS NC1: 5'-rCrGrUrUrArArUrCrGrCrGrUrArUrArArUrArCrGrCrGrUAT-3', 3'-rArUrArCrGrCrGrUrArUrArUrArCrGrCrGrArUrUrArArCrGrArC-5') [74] were diluted in RNase-free water to 0.2 µg/µl. After morphine minipump implantation and acute nociceptive behavior on D0 in rats, the first dose of *S1pr1*-targeting or non-targeting sequence (10 µl of 0.2 µg/µl) was administered via intrathecal catheters. Administration of siRNA sequences was repeated again on D1, D2, and D4 post-minipump implantation.

Development of morphine-induced thermal hyperalgesia and antinociceptive tolerance in rats.

Rats were lightly anesthetized with 3% isoflurane, maintained on 2% isoflurane in 100% O₂ and an osmotic minipump (Alzet 2001; Alzet Osmotic Pumps, Cupertino CA, USA) primed to deliver 1.0 µl/h saline vehicle or morphine at 75 µg/µl/h (~8.2–9 mg/kg/d) over seven days

was subcutaneously implanted in the interscapular region as described previously [53]. After implantation the animals were singly-housed for the remainder of the experiment.

Thermal hyperalgesia: The development of thermal hyperalgesia during the seven day infusion of morphine was measured in rats by the Hargreaves method [29] using a Basile Plantar Test (Ugo Basile Model 37370; Monvalle VA, Italy) with a cutoff latency of 20 s to prevent tissue damage, as previously described [53]. A significant ($P<0.05$) reduction in paw-withdrawal latency (PWL) over the infusion period time compared to baseline is characterized as thermal hyperalgesia.

Mechano-allodynia: Mechano-allodynia was assessed by probing the plantar aspect of the hind paw with calibrated von Frey filaments (Stoelting, Wood Dale, IL, USA; mice: 0.04–2.00 g; rats: 1.4–26 g) according to the “up-and-down” method [19] and a paw withdrawal threshold (PWT, g) was calculated, as previously described [35].

Antinociceptive tolerance: Rats received acute intraperitoneal injections of morphine (6 mg/kg) during the period of infusion with morphine or saline on days 1, 3 and 6 [53]; nociceptive responses were measured using the tail-flick assay [16] 30 minutes after the acute injection of morphine (time period was demonstrated previously to be the time of maximal antinociception at this dose) [53]. The latencies for tail withdrawal from a noxious radiant heat source (Ugo Basile Model 37360; Monvalle VA, Italy) were measured to determine the changes in the antinociceptive effect of the acute morphine challenge as previously described [53]. The cutoff latencies (rats: 10 sec and mice: 15 sec) were set to prevent tissue injury and the heat intensity was set to elicit a 2–4 sec baseline withdrawal latency. Tolerance to the morphine antinociceptive effect was indicated by a significant ($P<0.05$) reduction in tail-flick latencies 30 min after the acute morphine challenge. Data are reported as the percentage of maximal possible antinociceptive effect (%MPE) with 100% being complete morphine antinociception as calculated by the following equation:

$$\% \text{MPE} = (\text{response latency} - \text{baseline latency}) / (\text{cutoff latency (10 or 15 sec)} - \text{baseline latency}) \times 100.$$

Chronic Constriction Injury Model.

Chronic constriction injury (CCI) to the sciatic nerve of the left hind leg in male mice was performed under general anaesthesia using the well-characterized Bennett model [3]. Briefly, CD-1 mice rats were anesthetized with 3% isoflurane/O₂ and maintained on 2% isoflurane/O₂ during surgery. A small incision (1–1.5 cm in length) was made in the middle of the lateral aspect of the left thigh to expose the sciatic nerve, which was loosely ligated around the entire diameter of the nerve at two distinct sites (spaced 1 mm apart) using silk sutures (6.0). Mechano-allodynia was assessed by probing the plantar aspect of the hind paw with calibrated von Frey filaments (Stoelting, Wood Dale, IL, USA; mice: 0.04–2.00 g; rats: 1.4–26 g) according to the “up-and-down” method [19] and a paw withdrawal threshold (PWT, g) was calculated, as previously described [35]. Beginning on d7 (peak CCI-induced mechano-allodynia), mice were treated with an intraperitoneal injection of morphine (6 mg/kg, once daily) and mechano-allodynia was measured prior to and following morphine injection. The data are expressed as a percentage of expected reversal (%Reversal) using the

following equation: $\% \text{Reversal} = (\text{PWT}_{\text{g}_{1\text{h}}} - \text{PWT}_{\text{g}_{\text{BL}}}) / (\text{PWT}_{\text{g}_{\text{d0}}} - \text{PWT}_{\text{g}_{\text{BL}}})$, where $\text{PWT}_{\text{g}_{1\text{h}}}$ = paw withdrawal threshold in grams at 1h post morphine; $\text{PWT}_{\text{g}_{\text{BL}}}$ = paw withdrawal threshold in grams prior to morphine and $\text{PWT}_{\text{g}_{\text{d0}}}$ = paw withdrawal threshold in grams at d0 before CCI.

Morphine-induced persistent sensitization.

Male F344 rats underwent CCI surgery and beginning on day 10 post CCI [3], animals received subcutaneous injections of saline or morphine (5 mg/kg/ml, twice daily) and intraperitoneal injections of S1PR1 antagonists or their vehicle once a day for five days. Mechano-allodynia behavior was measured before and 10 days after surgery and followed for 8 weeks by probing the distal region of the heel in the hind paws within the region of sciatic innervation with calibrated von Frey filaments (0.40 g-15.14 g). Absolute threshold (the 50% probability of response) was calculated from behavioral responses by fitting a Gaussian integral psychometric function using a maximum-likelihood fitting method [30; 72], as described previously [47; 48].

Defining estrous cycle stage.

Given the multi-day nature of the design in freely cycling females, a vaginal smear was taken after the last behavioral time point and stage of estrous defined by cytology as described [8]. All animals displayed a normal 4–5 day estrous cycle.

Western blot.

The lower lumbar enlargement of the male rat spinal cords (L4-L6) were harvested, flash frozen in liquid nitrogen, and stored at -80°C . Samples were homogenized in extraction buffer [10 mM HEPES, pH 7.9; 10 mM KCl; 0.1 mM EGTA; 0.1 mM EDTA; 1 mM DTT; 0.5 mM PMSF; 15 $\mu\text{g}/\text{ml}$ trypsin inhibitor; 3 $\mu\text{g}/\text{ml}$ pepstatin A, 2 $\mu\text{g}/\text{ml}$ leupeptin, 40 $\mu\text{g}/\text{ml}$ benzamidine; 1 mM sodium orthovanadate] and the cytosolic and nuclear fractions were isolated as previously described [22]. The nuclear pellet was lysed in nuclear extraction buffer [1% Triton X-100, 150 mM NaCl, 10 mM tris-HCl pH 7.4, 1 mM ethylene glycol tetraacetic acid (EGTA), 1 mM ethylenediaminetetraacetic acid (EDTA), 0.2 mM PMSF, 20 μM leupeptin, 0.2 mM sodium orthovanadate]. Protein concentrations in both cytosolic and nuclear fractions were measured by bicinchoninic acid assay (Thermo Fisher Scientific, Carlsbad CA, USA). Fractions were subjected to 10% or 12% SDS-polyacrylamide gel electrophoresis (SDS-PAGE) and electrotransferred to nitrocellulose membranes to measure I κ B- α (1:1000; Santa Cruz Biotechnology sc-1643, Santa Cruz CA, USA), p-p38 (1:500; SantaCruz Biotechnology sc-17852-R, Santa Cruz CA, USA), total p38 (1:500; SantaCruz Biotechnology sc-81621, Santa Cruz CA, USA), GFAP (1:500; SantaCruz Biotechnology sc-6170, Santa Cruz CA, USA) and OX-42 (ab1211 Abcam). The membranes were blocked in 5% (w/v) non-fat milk in PBS and washed with 1X PBS-T. Immunolabeled proteins were visualized with peroxidase-conjugated bovine anti-mouse immunoglobulin G (IgG) secondary antibody or goat anti-rabbit IgG (1:2000, Jackson ImmunoResearch, West Grove PA, USA) and enhanced chemiluminescence (ECL) detection system reagent, according to the manufacturer's instructions (SuperSignal West Pico Chemiluminescent Substrate, Thermo Fisher Scientific, Carlsbad CA, USA). Relative protein expression was quantified by band densitometry with Chemidoc XRS+ Documentation System Bio-Rad software.

Each membrane was stripped and subsequently probed for β -actin (for cytosolic extract) or lamin A (for nuclear extract) proteins (1:10000; SantaCruz Biotechnology sc-6215, Santa Cruz CA, USA) for use as endogenous loading controls. All densitometry data are normalized to β -actin or lamin A bands.

Adjustments to blot image for publication were limited to linear brightness and contrast or color inversion using Image J v.1.47 [66] where noted. All blot images were cropped for the clarity of data presentation

Cytokine ELISA.

The levels of cytokines in spinal cord lysates were assessed using commercially available ELISA kits (R&D Systems, Minneapolis MN, USA) according to manufacturer's protocol.

Morphine analysis by quantitative Liquid Chromatography-Mass Spectrometry/Mass Spectrometry-Multiple Reaction Monitoring (LC-MS/MS-MRM).

Morphine concentrations were determined at Mallinckrodt Pharmaceuticals from 25 μ L plasma using methods previously described (Kole et al., 2011; Zou et al., 2009). LC-MS/MS analysis was performed on a Waters Acquity UPLC system connected to a Sciex API 4000 Q-Trap Mass Spectrometer utilizing the Turbo Ion Spray source in positive ion multiple reaction monitoring mode. Analyst version 1.6 was used to calculate concentrations of analytes which were reported in ng/ml.

Determining ED₅₀ values.

The ED₅₀ and the corresponding 95% confidence interval (95% CI) were determined by curve-fitting the %MPE as described [53] or %Prevention of thermal hyperalgesia using the least sum of square method by a normalized 3-parameter, non-linear analysis (Hill-slope =1). %Prevention of thermal hyperalgesia on D6 = $(PWL_{\text{group}} - \text{mean } PWL_{\text{Veh+Mor}}) / (PWL_{\text{Veh+Sal}} - \text{mean } PWL_{\text{Veh+Mor}}) \times 100$.

Statistics.

Data are expressed as mean \pm SD (standard deviation) or SEM (standard error of the mean) for N animals as noted. Data were analyzed by two-tailed, one-way ANOVA with Dunnett's comparisons or two-way ANOVA with Bonferroni comparisons as noted. Differences between non-linear curves for ED₅₀ values were analyzed by Extra sum-of-squares F test. All data were analyzed using GraphPad Prism (versions 5.00–8.0.1 for Windows, GraphPad Software, San Diego CA USA, www.graphpad.com). False discovery rate was determined by Benjamini-Hochberg method using SPSS (IBM; version 24.0.0.0). Significant differences were defined at P<0.05.

Results

S1PR1 signaling in the spinal cord contributes to the development of OIH and tolerance.

In agreement with our previous study [53], subcutaneous infusion of morphine, but not saline, in male rats that was delivered by primed osmotic minipumps over seven days led to a time-dependent reduction in paw withdrawal latency (PWL, seconds) (Fig. 1A) by day

three that lasted until the end of the study (day six), indicating the development of thermal hyperalgesia. Reductions in tail flick latencies after a challenge with an acute intraperitoneal dose of morphine [53] also occurred in morphine-infused rats over the same time frame (Fig. 1B), indicating the development of antinociceptive tolerance. Blocking S1PR1 signaling with daily intrathecal injections of the selective S1PR1 antagonist W146, but not its inactive enantiomer W140 [4], blocked OIH and antinociceptive tolerance in a dose-dependent manner (Figs. 1A,B). W146 had no effect in saline-treated rats (Figs. 1A,B). In contrast to its effects on OIH and antinociceptive tolerance, W146 did not significantly alter antinociceptive effects evoked by an acute injection of morphine ($F(1,28)=0.06$, $p=0.81$; Fig. 2) in male rats, establishing that blocking S1PR1 does not enhance acute responses to morphine. The ED_{50} values (the dose that yields 50% effect) of an acute dose of morphine in naïve rats treated with intrathecal W146 was 1.9 mg/kg; 95%CI:1.1–3.2; while those treated with vehicle was 1.7 mg/kg; 95%CI:1.1–2.

In contrast to S1PR1 antagonists, intrathecal administration of the S1PR2 antagonist JTE-013 [63] and the S1PR3 antagonist CAY10444 [63] did not block the development of hyperalgesia, while both had a modest effect on tolerance in male rats (Fig. 3). The doses used for these antagonists block S1PR subtypes 2 or 3 and higher doses were avoided due to documented spill-over effects at other S1PRs [63]. S1PR4 and 5 were not investigated, since S1PR4 is not expressed in the spinal cord and S1PR5 is mainly expressed in oligodendrocytes [64], which are not recognized as key players in opioid-induced adverse effects.

Our data suggest that S1PR1 in the spinal cord plays an important role in transducing the effects of S1P signaling in the development of OIH and antinociceptive tolerance guiding further investigations that focused on this receptor subtype. This was examined further through additional pharmacological and genetic approaches. Intrathecal administration of NIBR-14 significantly blocked OIH and antinociceptive tolerance in male rats (Figs. 4A,B). NIBR-14 had no effect in saline-treated rats (Figs. 4A,B). NIBR-14 is a methyl ester pro-drug that is rapidly hydrolyzed *in vivo* to the carboxylic acid NIBR-15, which is a potent and highly selective competitive S1PR1 antagonist that is structurally distinct from W146 [1].

The pharmacological effects of S1PR1 antagonists were validated further using RNA silencing of *S1pr1*. We have previously shown a greater than 45% reduction in S1PR1 protein levels in the dorsal horn of the spinal cord with intrathecal injections of our *S1pr1*-targeting siRNA (small interfering RNA, si*S1pr1*) sequence [69]. Using this sequence, we found that it recapitulated the pharmacological effects obtained with W146 and NIBR-14 on OIH and antinociceptive tolerance in male rats (Fig. 5).

To strengthen our findings and increase rigor, we profiled the pharmacological profiles of several competitive and functional S1PR1 antagonists NIBR-14/NIBR-15, FTY720 and ponesimod given orally (a preferred clinical regimen). In contrast to the highly selective S1PR1 antagonists NIBR-14/NIBR-15 [1], FTY720 (once phosphorylated by sphingosine kinase 2 to the biologically active FTY720-P) and ponesimod are S1PR agonists that act as functional S1PR1 antagonists by potently and irreversibly reducing S1PR1 levels at the plasma membrane [6]. These functional antagonists stand in stark contrast to the endogenous

ligands (e.g., S1P) or the highly selective S1PR1 agonist SEW2871 that allow S1PR1 to recycle back to the plasma membrane [4]. Oral delivery of NIBR-14 in male rats prevented OIH and antinociceptive tolerance (Figs. 6A,B). The ED₅₀ for NIBR-14 was 1.8 μmol/kg/day [95% confidence interval (CI) 1–3 μmol/kg/day] for hyperalgesia and 1.7 μmol/kg/day [95% CI 1–3] for tolerance. Consistent with the NIBR-14, the *in vivo* carboxylic acid form, NIBR15, blocked OIH and tolerance (Figs. 6A,B). These effects were mimicked by FTY720 (Figs. 6C,D) or ponesimod (Figs. 6E,F). The ED₅₀ for FTY720 was 0.08 μmol/kg/day [95% CI 0.05–1 μmol/kg/day] for hyperalgesia and 0.09 μmol/kg/day [95% CI 0.06–1] for tolerance. FTY720 also blocked OIH and antinociceptive tolerance in female rats (Figs. 6G,H). NIBR-14, FTY720 and ponesimod had no effects in rats infused with saline alone (Figs. 6A–F).

In contrast to the effects of observed with intrathecal or systemic administration of functional or competitive S1PR1 antagonists intrathecal or systemic delivery of the S1PR1 agonist, SEW2871 failed to block OIH and tolerance in male rats (Figs. 4A,B). The maximal dose of SEW2871 tested was 20 mg/kg. Higher doses of SEW2871 were not tested since 20 mg/kg is a high dose known to cause lymphopenia [9; 20; 65].

S1PR1 antagonists attenuate the development of morphine-induced anti-allodynic tolerance in a model of neuropathic pain.

We investigated whether S1PR1 antagonists retain their ability to block morphine-induced anti-allodynic tolerance in the context of nerve injury. In mice with traumatic nerve injury-induced neuropathic pain caused by chronic constriction of the sciatic nerve (CCI), mechano-allodynia peaks by day seven post-surgery [3]. Subcutaneous injection of morphine on day seven reversed mechano-allodynia by approximately 90% (Fig. 7), but these effects diminished after four to five days of morphine injections, indicating the development of anti-allodynic tolerance. NIBR-15 or FTY720 completely blocked the development of anti-allodynic tolerance (Fig. 7A). At these doses, NIBR-15 or FTY720 do not attenuate or block CCI-induced neuropathic pain and therefore we did not include these groups in our studies [9]. LC-MS/MS-MRM revealed the plasma levels of morphine metabolites (Fig. 7B) in mice treated with morphine and NIBR-15 or FTY720 were not significantly different from mice treated with morphine and vehicle; suggesting that beneficial effects of S1PR1 antagonists are not due to alterations in morphine pharmacokinetics.

S1PR1 antagonists attenuate the development of morphine-induced persistent neuropathic pain.

In addition to the eventual reduction of antinociceptive efficacy of morphine in managing neuropathic pain from extended use, there is evidence that opioid usage can adversely affect the underlying neuropathic pain state [32]. We have reported that the neuropathic pain state begins to resolve itself three to four weeks after traumatic nerve injury. However, a brief five-day use of opioids following injury caused persistent sensitization that prolonged the neuropathic pain state as long as eight weeks [25]. Consistent with these findings, a brief five-day exposure to morphine significantly extended CCI-induced mechano-allodynia in

rats (Fig. 8). Yet, when FTY720 was co-administered with morphine, persistent sensitization was significantly attenuated (Fig. 8). FTY720 alone had no effect (Fig. 8).

S1PR1 antagonists reduce astrocyte and microglia reactivity and neuroinflammation in the dorsal horn of the spinal cord.

The CNS effects of S1PR1 antagonists in animal models of multiple sclerosis [6; 11] and pain [9; 22; 26; 35; 69] have been attributed in part to their effects on neuroinflammation. Glial activation and neuroinflammation in the CNS have emerged as key contributors to the development of opioid-induced hyperalgesia [61] and antinociceptive tolerance [67]. We found that expression of markers associated with gliosis and enhanced astrocyte (glial fibrillary acidic protein, GFAP; astrocytes) and microglia (CD11b/c, clone OX-42; microglia) reactivity (Figs. 9A,B and 10,B) were increased in the dorsal spinal cord of morphine-treated rats when compared to animals that received saline infusion over the same time period. These effects were blocked by intrathecal W146 (Figs. 9A,B) or oral FTY720 (Figs. 10A,B) treatment. Moreover, we found evidence of active neuroinflammatory processes that have been reported with OIH and tolerance [21; 24; 33; 34; 41; 52; 75; 76]. In animals treated with morphine, p38 phosphorylation (Figs. 9C and 10C) and nuclear factor κ B (NF κ B) activation [reduced I κ B α and increased nuclear NF κ B-p65; Figs. 9D and 10D] increased in the dorsal horn of the spinal cord as did the production of inflammatory, pro-nociceptive IL-1 β and associated cytokines [TNF (tumor necrosis factor) and IL-6 (interleukin-6)] (Fig. 11A). The morphine-induced effects were blocked in rats treated with intrathecal W146 or oral FTY720 (Figs. 9–11). In contrast, the expression of the potent and anti-inflammatory and neuroprotective cytokine, IL-10 (interleukin-10) [44] was increased in the dorsal horn of the spinal cord of rats treated with W146 and FTY720 treatment during morphine but not saline-infusion (Fig. 11B).

Discussion

There is a desperate need for an opioid adjunct therapy to improve the long-term use of opioids in chronic pain. Using several diverse functional and competitive S1PR1 antagonists, we provide evidence that the activation of S1PR1 signaling is germane to the development of OIH and antinociceptive tolerance.

Our identification of S1PR1 as a critical receptor subtype in the effects of morphine-induced S1P is highly exciting as a potential therapeutic target to mitigate opioid-induced adverse effects. The functional S1PR1 antagonist, FTY720, is already FDA approved for the treatment of multiple sclerosis [6] and other S1PR1 functional antagonists, such as siponimod and ponesimod, are in advanced clinical trials for multiple sclerosis. Selective S1PR1 antagonists, such as NIBR-15, are also in preclinical development [4]. Once the involvement of S1P/S1PR1 signaling pathways is validated in the clinical manifestations of OIH and tolerance, the re-purposing of these S1PR1 antagonists for mitigating opioid adverse effects should prove an exciting approach to address this unmet medical need. Moreover, our results provide support for findings in other models of disease where functional antagonism of S1PR1 rather than persistent agonism/signaling at S1PR1 was identified as the mechanism of action of FTY720 and ponesimod [4; 9; 15; 26; 35; 68; 69].

Indeed, their pharmacological profiles mimicked those obtained with selective S1PR1 antagonists, but contrasted those obtained with the S1PR1 agonist, SEW2871.

We found little evidence to support a role for S1PR2 or S1PR3 in OIH. S1PR2 and S1PR3 antagonism did have a modest, but significant, effect on morphine-induced antinociceptive tolerance; suggesting they may provide some contribution to the development of this adverse effect. S1PR2 [14; 79] and S1PR3 [23; 79] are expressed on astrocytes and microglia. S1PR3 can contribute to neuro-inflammatory processes [23] and S1PR2 can alter the blood-brain barrier to affect neuroinflammation [14]. However, FTY720 [6] and ponesimod [58], which do not bind S1PR2, were able to block OIH and tolerance; suggesting the contribution of S1PR2 to morphine-induced effects are minimal. As more selective S1PR3 antagonists become available, additional studies will need to be done to fully understand the role S1PR3 in opioid-induced adverse effects.

Our results also reveal that S1PR1 contributes to the development of neuroinflammatory events in the spinal cord associated with morphine-induced S1P signaling. A growing body of evidence now supports the notion that sustained morphine drives glial activation and causes an imbalance between inflammatory signaling from cytokines such as IL-1 β and anti-inflammatory cytokine signaling through IL-10 [24; 34; 61]. Several triggers have been proposed including direct activation of toll-like receptors on glia by morphine and glial response to increased ATP in the synapse [24; 34; 61]. In turn, this imbalance towards inflammatory signaling leads to increased neuronal excitability and long-term potentiation in the CNS [24; 34; 61]. S1PR1 expression increases during neuroinflammation and its expression is associated with reactive microglia and astrocytes [31; 42]. Moreover, its activity in astrocytes [11; 51; 55; 62] and microglia [49; 54; 59] contributes to their increased reactivity and migration [11; 49; 51; 59], activation of NF κ B [62] and induction of cytokine and chemokine production [11; 54; 55; 62]. Accordingly, the functional and competitive S1PR1 antagonists used in our studies blocked increased expression of markers of gliosis and astrocyte and microglia reactivity, the activation of NF κ B and p38 kinase signaling pathways and the increase production of inflammatory cytokines during sustained morphine treatment. Moreover, IL10 levels increased in the spinal cord in response to treatment with S1PR1 antagonists, which has been shown as part of the way S1PR1 antagonists attenuate or resolve inflammation in other diseases including colitis [17], chemotherapy-induced neuropathic pain [35; 69], multiple sclerosis [11; 62], autoimmune diabetes [36] and corneal allograft rejection [80]. Emerging evidence now suggests that astrocyte-derived S1PR1 signaling is a critical driver of neuroinflammation [4; 11; 22; 55; 62; 69] and the activation and S1P-dependent proinflammatory effects in microglia are secondary to S1PR1-mediated effects in astrocytes [11; 62]. Consistent with this, we have recently found intrathecal administration of SEW2871 induces mechano-hypersensitivities in normal rats through NLRP3/IL-1 β -dependent neuroinflammation and astrocyte-specific signaling [22]. Given these proinflammatory effects of astrocyte-specific S1PR1, coupled with evidence that S1PR1 expression in the CNS is greatest in astrocyte populations [79] and increases in CNS astrocytes during neuroinflammation [31], it is possible that astrocytes are the cellular substrate for that actions of S1P and S1PR1 antagonist during the development of OIH and tolerance. Whether S1PR1 expression in astrocytes is increased following morphine and contributes to these adverse effects is a subject of ongoing

investigation in our laboratories. The impact of S1PR1 antagonists in blocking neuroinflammatory processes in the spinal cord were obtained after intrathecal or oral administration of the drugs and we cannot exclude the potential involvement of S1PR1 effects in dorsal root ganglia due to potential drug access at this site post intrathecal injection [39], which is a limitation of intrathecal routes. Accordingly, additional beneficial effects of S1PR1 antagonists may include their inhibitory effects of neuronal S1PR1 activity in dorsal root ganglia [40; 78].

Until recently, OIH has only been assessed concurrently with or within a few hours after opioid administration and largely in absence of an exaggerated pain state [25]. Our data provide evidence that the development of morphine anti-allodynic tolerance in a model of traumatic nerve injury and the persistent sensitization enabled by a brief exposure to the opioid can be prevented by an S1PR1 antagonist. This suggests that S1PR1 signaling contributes to neuropathological changes involved in the development of anti-allodynic tolerance and persistent sensitization. Although we have shown that S1PR1 antagonists are capable of reversing CCI-induced neuropathic pain, their effects on the anti-allodynic effects of morphine occurred with doses of S1PR1 antagonist that had no effect on CCI-induced neuropathic pain when used alone [9]. Here it is possible that there is synergism between morphine's anti-allodynic effects and S1PR1 antagonists' effects on CCI-induced neuroinflammation that provide neuropathic pain relief. However, our findings in our persistent pain model may suggest that S1PR1 antagonist are addressing the neuroinflammation brought on by morphine administration and not necessarily the underlying changes brought on by CCI. Evidence suggests that 5 days of morphine will increase spinal glial cell reactivity and NLRP3-driven neuroinflammation over that brought on by CCI [25]. This increase in neuroinflammation is what is thought to drive the development and maintenance of persistent sensitization [25]. Yet, we found no evidence that FTY720, when used alone, hastened the recovery of animals from CCI-induced neuropathic pain when compared to animals treated with vehicle and saline. This suggests that at low doses, FTY720 are attenuating the neuroinflammatory effects triggered by morphine. Additional pharmacological and biochemical studies will be needed to determine how these pathways interact in neuropathic pain models.

The mechanisms by which sustained exposure to morphine triggers sphingolipid metabolism are not known. Activation of classical (μ -opioid receptor) [13; 50; 57; 61] and non-classical (toll-like receptor 4, TLR4) pathways on glial cells [76] contribute to opioid-induced antinociceptive tolerance and OIH. Sphingolipid composition, particularly the concentration of ceramide, has been shown to be important for the organization of μ -opioid receptor lipid microdomains [46] and there is some evidence suggesting a link between μ -opioid receptor activation and increased ceramide production [60]. In addition, opioid-induced μ -opioid receptor internalization activates the NADH/NADPH oxidase system to contribute to oxidative stress [37], which, in turn, can stimulate sphingolipid metabolism [77]. However, activation of TLR4 has also been reported to activate the ceramide metabolic pathway [64]. Ongoing studies in our laboratories are addressing these questions.

Collectively, our findings provide compelling evidence that chronic morphine-induced alterations in sphingolipid metabolism and signaling through S1PR1 are germane to multiple

opioid-induced adverse events. Thus, this paradigm shift in the understanding of S1PR1 signaling has implications on the future development of S1PR1 antagonists as adjuncts to opioids for chronic pain treatment. Our work provides support for investigating the clinical validation of S1PR1 in opioid-induced adverse effects and considering the repurposing FTY720 as an opioid adjunct to mitigate adverse effects. More broadly, it is interesting to hypothesize that alterations in opioid-mediated sphingolipid metabolism within the central nervous system may also have implications on the development of the comorbidities associated with chronic opioid use, such as depression [27]. To this end, emerging evidence in other fields has linked depression to altered sphingolipid metabolism [7; 18].

Acknowledgements.

We thank Joe McClurg (Mallinkrodt Pharmaceuticals) for plasma M3G/M6G analysis and Leesa Bryant (Saint Louis University) for technical assistance.

Funding: This work was supported by grants from the National Institute of Drug Abuse (R21DA023056; Dr. Salvemini and RO1DA043543; Drs. Salvemini, Spiegel and Vanderah), Saint Louis University President's Research Fund (Dr. Salvemini) and University of Arizona Start-Up Funds (Dr. Vanderah).

Dr. Salvemini has patents submitted by Saint Louis University that cover some of the intellectual property described in this manuscript (U.S. patent number 8,747,844 and its divisional, U.S. patent number 8,945,549).

References

- [1]. Angst D, Janser P, Quancard J, Buehlmayr P, Berst F, Oberer L, Beerli C, Streiff M, Pally C, Hersperger R, Bruns C, Bassilana F, Bollbuck B. An oral sphingosine 1-phosphate receptor 1 (S1P(1)) antagonist prodrug with efficacy in vivo: discovery, synthesis, and evaluation. *Journal of medicinal chemistry* 2012;55(22):9722–9734. [PubMed: 23067318]
- [2]. Angst MS, Clark JD. Opioid-induced hyperalgesia: a qualitative systematic review. *Anesthesiology* 2006;104(3):570–587. [PubMed: 16508405]
- [3]. Bennett GJ, Xie YK. A peripheral mononeuropathy in rat that produces disorders of pain sensation like those seen in man. *Pain* 1988;33(1):87–107. [PubMed: 2837713]
- [4]. Bigaud M, Guerini D, Billich A, Bassilana F, Brinkmann V. Second generation S1P pathway modulators: research strategies and clinical developments. *Biochim Biophys Acta* 2014;1841(5):745–758. [PubMed: 24239768]
- [5]. Bolli MH, Abele S, Binkert C, Bravo R, Buchmann S, Bur D, Gatfield J, Hess P, Kohl C, Mangold C, Mathys B, Menyhart K, Muller C, Nayler O, Scherz M, Schmidt G, Sippel V, Steiner B, Strasser D, Treiber A, Weller T. 2-imino-thiazolidin-4-one derivatives as potent, orally active S1P1 receptor agonists. *Journal of medicinal chemistry* 2010;53(10):4198–4211. [PubMed: 20446681]
- [6]. Brinkmann V, Billich A, Baumruker T, Heining P, Schmouder R, Francis G, Aradhye S, Burtin P. Fingolimod (FTY720): discovery and development of an oral drug to treat multiple sclerosis. *Nature reviews* 2010;9(11):883–897.
- [7]. Brunkhorst-Kanaan N, Klatt-Schreiner K, Hackel J, Schroter K, Trautmann S, Hahnefeld L, Wicker S, Reif A, Thomas D, Geisslinger G, Kittel-Schneider S, Tegeder I. Targeted lipidomics reveal derangement of ceramides in major depression and bipolar disorder. *Metabolism* 2019;95:65–76. [PubMed: 30954559]
- [8]. Byers SL, Wiles MV, Dunn SL, Taft RA. Mouse estrous cycle identification tool and images. *PLoS one* 2012;7(4):e35538.
- [9]. Chen Z, Doyle TM, Luongo L, Largent-Milnes TM, Giancotti LA, Kolar G, Squillace S, Boccella S, Walker JK, Pendleton A, Spiegel S, Neumann WL, Vanderah TW, Salvemini D. Sphingosine-1-phosphate receptor 1 activation in astrocytes contributes to neuropathic pain. *Proceedings of the National Academy of Sciences of the United States of America* 2019;116(21):10557–10562. [PubMed: 31068460]

- [10]. Choi JW, Chun J. Lysophospholipids and their receptors in the central nervous system. *Biochimica et biophysica acta* 2013;1831(1):20–32. [PubMed: 22884303]
- [11]. Choi JW, Gardell SE, Herr DR, Rivera R, Lee CW, Noguchi K, Teo ST, Yung YC, Lu M, Kennedy G, Chun J. FTY720 (fingolimod) efficacy in an animal model of multiple sclerosis requires astrocyte sphingosine 1-phosphate receptor 1 (S1P1) modulation. *Proceedings of the National Academy of Sciences of the United States of America* 2011;108(2):751–756. [PubMed: 21177428]
- [12]. Collett BJ. Opioid tolerance: the clinical perspective. *British journal of anaesthesia* 1998;81(1):58–68. [PubMed: 9771273]
- [13]. Corder G, Tawfik VL, Wang D, Sypek EI, Low SA, Dickinson JR, Sotoudeh C, Clark JD, Barres BA, Bohlen CJ, Scherrer G. Loss of mu opioid receptor signaling in nociceptors, but not microglia, abrogates morphine tolerance without disrupting analgesia. *Nature medicine* 2017;23(2):164–173.
- [14]. Cruz-Orengo L, Daniels BP, Dorsey D, Basak SA, Grajales-Reyes JG, McCandless EE, Piccio L, Schmidt RE, Cross AH, Crosby SD, Klein RS. Enhanced sphingosine-1-phosphate receptor 2 expression underlies female CNS autoimmunity susceptibility. *The Journal of clinical investigation* 2014;124(6):2571–2584. [PubMed: 24812668]
- [15]. Cuzzocrea S, Doyle T, Campolo M, Paterniti I, Esposito E, Farr SA, Salvemini D. Sphingosine 1-Phosphate Receptor Subtype 1 as a Therapeutic Target for Brain Trauma. *Journal of neurotrauma* 2018;35(13):1452–1466. [PubMed: 29310513]
- [16]. D'Amour FE, Smith DL. A method for determining loss of pain sensation. *J Pharmacol Exp Ther* 1941;72(1):74–79.
- [17]. Daniel C, Sartory N, Zahn N, Geisslinger G, Radeke HH, Stein JM. FTY720 ameliorates Th1-mediated colitis in mice by directly affecting the functional activity of CD4+CD25+ regulatory T cells. *Journal of immunology* 2007;178(4):2458–2468.
- [18]. Dinoff A, Herrmann N, Lanctot KL. Ceramides and depression: A systematic review. *J Affect Disord* 2017;213:35–43. [PubMed: 28189963]
- [19]. Dixon WJ. Efficient analysis of experimental observations. *Annu Rev Pharmacol Toxicol* 1980;20:441–462. [PubMed: 7387124]
- [20]. Dong J, Wang H, Wu G, Zhao J, Zhang L, Zuo L, Zhu W, Gong J, Li Y, Gu L, Li J. Oral treatment with SEW2871, a sphingosine-1-phosphate type 1 receptor agonist, ameliorates experimental colitis in interleukin-10 gene deficient mice. *Clin Exp Immunol* 2014;177(1):94–101. [PubMed: 24611843]
- [21]. Doyle T, Esposito E, Bryant L, Cuzzocrea S, Salvemini D. NADPH-oxidase 2 activation promotes opioid-induced antinociceptive tolerance in mice. *Neuroscience* 2013;241:1–9. [PubMed: 23454539]
- [22]. Doyle TM, Chen Z, Durante M, Salvemini D. Activation of Sphingosine-1-Phosphate Receptor 1 in the Spinal Cord Produces Mechanohypersensitivity Through the Activation of Inflammasome and IL-1beta Pathway. *The journal of pain : official journal of the American Pain Society* 2019;20(8):956–964.
- [23]. Dusaban SS, Chun J, Rosen H, Purcell NH, Brown JH. Sphingosine 1-phosphate receptor 3 and RhoA signaling mediate inflammatory gene expression in astrocytes. *J Neuroinflammation* 2017;14(1):111. [PubMed: 28577576]
- [24]. Grace PM, Maier SF, Watkins LR. Opioid-induced central immune signaling: implications for opioid analgesia. *Headache* 2015;55(4):475–489. [PubMed: 25833219]
- [25]. Grace PM, Strand KA, Galer EL, Urban DJ, Wang X, Baratta MV, Fabisiak TJ, Anderson ND, Cheng K, Greene LI, Berkelhammer D, Zhang Y, Ellis AL, Yin HH, Campeau S, Rice KC, Roth BL, Maier SF, Watkins LR. Morphine paradoxically prolongs neuropathic pain in rats by amplifying spinal NLRP3 inflammasome activation. *Proceedings of the National Academy of Sciences of the United States of America* 2016;113(24):E3441–3450. [PubMed: 27247388]
- [26]. Grenald SA, Doyle TM, Zhang H, Slosky LM, Chen Z, Largent-Milnes TM, Spiegel S, Vanderah TW, Salvemini D. Targeting the S1P/S1PR1 axis mitigates cancer-induced bone pain and neuroinflammation. *Pain* 2017;158(9):1733–1742. [PubMed: 28570482]

- [27]. Gros DF, Milanak ME, Brady KT, Back SE. Frequency and severity of comorbid mood and anxiety disorders in prescription opioid dependence. *Am J Addict* 2013;22(3):261–265. [PubMed: 23617869]
- [28]. Groves A, Kihara Y, Chun J. Fingolimod: direct CNS effects of sphingosine 1-phosphate (S1P) receptor modulation and implications in multiple sclerosis therapy. *J Neurol Sci* 2013;328(1–2):9–18. [PubMed: 23518370]
- [29]. Hargreaves K, Dubner R, Brown F, Flores C, Joris J. A new and sensitive method for measuring thermal nociception in cutaneous hyperalgesia. *Pain* 1988;32(1):77–88. [PubMed: 3340425]
- [30]. Harvey LO. Efficient estimation of sensory thresholds. *Behavior Research Methods, Instruments, & Computers* 1986;18(6):623–632.
- [31]. Healy LM, Antel JP. Sphingosine-1-Phosphate Receptors in the Central Nervous and Immune Systems. *Current drug targets* 2016;17(16):1841–1850. [PubMed: 26424391]
- [32]. Hoffman EM, Watson JC, St Sauver J, Staff NP, Klein CJ. Association of Long-term Opioid Therapy With Functional Status, Adverse Outcomes, and Mortality Among Patients With Polyneuropathy. *JAMA Neurol* 2017;74(7):773–779. [PubMed: 28531306]
- [33]. Hutchinson MR, Coats BD, Lewis SS, Zhang Y, Sprunger DB, Rezvani N, Baker EM, Jekich BM, Wieseler JL, Somogyi AA, Martin D, Poole S, Judd CM, Maier SF, Watkins LR. Proinflammatory cytokines oppose opioid-induced acute and chronic analgesia. *Brain Behav Immun* 2008;22(8):1178–1189. [PubMed: 18599265]
- [34]. Hutchinson MR, Shavit Y, Grace PM, Rice KC, Maier SF, Watkins LR. Exploring the neuroimmunopharmacology of opioids: an integrative review of mechanisms of central immune signaling and their implications for opioid analgesia. *Pharmacological reviews* 2011;63(3):772–810. [PubMed: 21752874]
- [35]. Janes K, Little JW, Li C, Bryant L, Chen C, Chen Z, Kamocki K, Doyle T, Snider A, Esposito E, Cuzzocrea S, Bieberich E, Obeid L, Petrache I, Nicol G, Neumann WL, Salvemini D. The development and maintenance of paclitaxel-induced neuropathic pain require activation of the sphingosine 1-phosphate receptor subtype 1. *The Journal of biological chemistry* 2014;289(30):21082–21097. [PubMed: 24876379]
- [36]. Jorns A, Rath KJ, Terbish T, Arndt T, Meyer Zu Vilsendorf A, Wedekind D, Hedrich HJ, Lenzen S. Diabetes prevention by immunomodulatory FTY720 treatment in the LEW.1AR1-iddm rat despite immune cell activation. *Endocrinology* 2010;151(8):3555–3565. [PubMed: 20501676]
- [37]. Koch T, Seifert A, Wu DF, Rankovic M, Kraus J, Borner C, Brandenburg LO, Schroder H, Hollt V. μ -opioid receptor-stimulated synthesis of reactive oxygen species is mediated via phospholipase D2. *J Neurochem* 2009;110(4):1288–1296. [PubMed: 19519662]
- [38]. Kunkel GT, Maceyka M, Milstien S, Spiegel S. Targeting the sphingosine-1-phosphate axis in cancer, inflammation and beyond. *Nature reviews* 2013;12(9):688–702.
- [39]. Ledebor A, Jekich BM, Sloane EM, Mahoney JH, Langer SJ, Milligan ED, Martin D, Maier SF, Johnson KW, Leinwand LA, Chavez RA, Watkins LR. Intrathecal interleukin-10 gene therapy attenuates paclitaxel-induced mechanical allodynia and proinflammatory cytokine expression in dorsal root ganglia in rats. *Brain Behav Immun* 2007;21(5):686–698. [PubMed: 17174526]
- [40]. Li C, Li JN, Kays J, Guerrero M, Nicol GD. Sphingosine 1-phosphate enhances the excitability of rat sensory neurons through activation of sphingosine 1-phosphate receptors 1 and/or 3. *J Neuroinflammation* 2015;12:70. [PubMed: 25880547]
- [41]. Little JW, Cuzzocrea S, Bryant L, Esposito E, Doyle T, Rausaria S, Neumann WL, Salvemini D. Spinal mitochondrial-derived peroxynitrite enhances neuroimmune activation during morphine hyperalgesia and antinociceptive tolerance. *Pain* 2013;154(7):978–986. [PubMed: 23590939]
- [42]. Liu H, Jin H, Yue X, Luo Z, Liu C, Rosenberg AJ, Tu Z. PET Imaging Study of S1PR1 Expression in a Rat Model of Multiple Sclerosis. *Mol Imaging Biol* 2016;18(5):724–732. [PubMed: 26975859]
- [43]. Liu H, Sugiura M, Nava VE, Edsall LC, Kono K, Poulton S, Milstien S, Kohama T, Spiegel S. Molecular cloning and functional characterization of a novel mammalian sphingosine kinase type 2 isoform. *The Journal of biological chemistry* 2000;275(26):19513–19520. [PubMed: 10751414]

- [44]. Lobo-Silva D, Carriche GM, Castro AG, Roque S, Saraiva M. Balancing the immune response in the brain: IL-10 and its regulation. *J Neuroinflammation* 2016;13(1):297. [PubMed: 27881137]
- [45]. Maceyka M, Spiegel S. Sphingolipid metabolites in inflammatory disease. *Nature* 2014;510(7503):58–67. [PubMed: 24899305]
- [46]. Marino KA, Prada-Gracia D, Provasi D, Filizola M. Impact of Lipid Composition and Receptor Conformation on the Spatio-temporal Organization of mu-Opioid Receptors in a Multi-component Plasma Membrane Model. *PLoS Comput Biol* 2016;12(12):e1005240.
- [47]. Milligan ED, Mehmert KK, Hinde JL, Harvey LO, Martin D, Tracey KJ, Maier SF, Watkins LR. Thermal hyperalgesia and mechanical allodynia produced by intrathecal administration of the human immunodeficiency virus-1 (HIV-1) envelope glycoprotein, gp120. *Brain research* 2000;861(1):105–116. [PubMed: 10751570]
- [48]. Milligan ED, O'Connor KA, Nguyen KT, Armstrong CB, Twining C, Gaykema RP, Holguin A, Martin D, Maier SF, Watkins LR. Intrathecal HIV-1 envelope glycoprotein gp120 induces enhanced pain states mediated by spinal cord proinflammatory cytokines. *The Journal of neuroscience : the official journal of the Society for Neuroscience* 2001;21(8):2808–2819. [PubMed: 11306633]
- [49]. Moon E, Han JE, Jeon S, Ryu JH, Choi JW, Chun J. Exogenous S1P Exposure Potentiates Ischemic Stroke Damage That Is Reduced Possibly by Inhibiting S1P Receptor Signaling. *Mediators of inflammation* 2015;2015:492659.
- [50]. Morgan MM, Christie MJ. Analysis of opioid efficacy, tolerance, addiction and dependence from cell culture to human. *British journal of pharmacology* 2011;164(4):1322–1334. [PubMed: 21434879]
- [51]. Mullershausen F, Craveiro LM, Shin Y, Cortes-Cros M, Bassilana F, Osinde M, Wishart WL, Guerini D, Thallmair M, Schwab ME, Sivasankaran R, Seuwen K, Dev KK. Phosphorylated FTY720 promotes astrocyte migration through sphingosine-1-phosphate receptors. *J Neurochem* 2007;102(4):1151–1161. [PubMed: 17488279]
- [52]. Muscoli C, Cuzzocrea S, Ndengele MM, Mollace V, Porreca F, Fabrizi F, Esposito E, Masini E, Matuschak GM, Salvemini D. Therapeutic manipulation of peroxynitrite attenuates the development of opiate-induced antinociceptive tolerance in mice. *J Clin Invest* 2007;117(11):3530–3539. [PubMed: 17975673]
- [53]. Muscoli C, Doyle T, Dagostino C, Bryant L, Chen Z, Watkins LR, Ryerse J, Bieberich E, Neumann W, Salvemini D. Counter-regulation of opioid analgesia by glial-derived bioactive sphingolipids. *The Journal of neuroscience : the official journal of the Society for Neuroscience* 2010;30(46):15400–15408. [PubMed: 21084596]
- [54]. Noda H, Takeuchi H, Mizuno T, Suzumura A. Fingolimod phosphate promotes the neuroprotective effects of microglia. *J Neuroimmunol* 2013;256(1–2):13–18. [PubMed: 23290828]
- [55]. O'Sullivan SA, O'Sullivan C, Healy LM, Dev KK, Sheridan GK. Sphingosine 1-phosphate receptors regulate TLR4-induced CXCL5 release from astrocytes and microglia. *J Neurochem* 2018;144(6):736–747. [PubMed: 29377126]
- [56]. Olivera A, Kohama T, Edsall L, Nava V, Cuvillier O, Poulton S, Spiegel S. Sphingosine kinase expression increases intracellular sphingosine-1-phosphate and promotes cell growth and survival. *J Cell Biol* 1999;147(3):545–558. [PubMed: 10545499]
- [57]. Pasternak GW, Pan Y-X. Mu opioids and their receptors: evolution of a concept. *Pharmacological reviews* 2013;65(4):1257–1317. [PubMed: 24076545]
- [58]. Piali L, Froidevaux S, Hess P, Nayler O, Bolli MH, Schlosser E, Kohl C, Steiner B, Clozel M. The selective sphingosine 1-phosphate receptor 1 agonist ponesimod protects against lymphocyte-mediated tissue inflammation. *J Pharmacol Exp Ther* 2011;337(2):547–556. [PubMed: 21345969]
- [59]. Quancard J, Bollbuck B, Janser P, Angst D, Berst F, Buehlmeier P, Streiff M, Beerli C, Brinkmann V, Guerini D, Smith PA, Seabrook TJ, Traebert M, Seuwen K, Hersperger R, Bruns C, Bassilana F, Bigaud M. A potent and selective S1P(1) antagonist with efficacy in experimental autoimmune encephalomyelitis. *Chem Biol* 2012;19(9):1142–1151. [PubMed: 22999882]

- [60]. Ritter JK, Fang Y, Xia M, Li PL, Dewey WL. Contribution of acid sphingomyelinase in the periaqueductal gray region to morphine-induced analgesia in mice. *Neuroreport* 2012;23(13):780–785. [PubMed: 22825003]
- [61]. Roeckel LA, Le Coz GM, Gaveriaux-Ruff C, Simonin F. Opioid-induced hyperalgesia: Cellular and molecular mechanisms. *Neuroscience* 2016;338:160–182. [PubMed: 27346146]
- [62]. Rothhammer V, Kenison JE, Tjon E, Takenaka MC, de Lima KA, Borucki DM, Chao CC, Wilz A, Blain M, Healy L, Antel J, Quintana FJ. Sphingosine 1-phosphate receptor modulation suppresses pathogenic astrocyte activation and chronic progressive CNS inflammation. *Proceedings of the National Academy of Sciences of the United States of America* 2017;114(8):2012–2017. [PubMed: 28167760]
- [63]. Salomone S, Waeber C. Selectivity and specificity of sphingosine-1-phosphate receptor ligands: caveats and critical thinking in characterizing receptor-mediated effects. *Frontiers in pharmacology* 2011;2:9. [PubMed: 21687504]
- [64]. Salvemini D, Doyle T, Kress M, Nicol G. Therapeutic targeting of the ceramide-to-sphingosine 1-phosphate pathway in pain. *Trends in pharmacological sciences* 2013;34(2):110–118. [PubMed: 23318139]
- [65]. Sanna MG, Liao J, Jo E, Alfonso C, Ahn MY, Peterson MS, Webb B, Lefebvre S, Chun J, Gray N, Rosen H. Sphingosine 1-phosphate (S1P) receptor subtypes S1P1 and S1P3, respectively, regulate lymphocyte recirculation and heart rate. *The Journal of biological chemistry* 2004;279(14):13839–13848. [PubMed: 14732717]
- [66]. Schneider CA, Rasband WS, Eliceiri KW. NIH Image to ImageJ: 25 years of image analysis. *Nat Methods* 2012;9(7):671–675. [PubMed: 22930834]
- [67]. Shen CH, Tsai RY, Shih MS, Lin SL, Tai YH, Chien CC, Wong CS. Etanercept restores the antinociceptive effect of morphine and suppresses spinal neuroinflammation in morphine-tolerant rats. *Anesthesia and analgesia* 2011;112(2):454–459. [PubMed: 21081778]
- [68]. Sim-Selley LJ, Wilkerson JL, Burston JJ, Hauser KF, McLane V, Welch SP, Lichtman AH, Selley DE. Differential Tolerance to FTY720-induced Antinociception in Acute Thermal and Nerve Injury Mouse Pain Models: Role of S1P Receptor Adaptation. *J Pharmacol Exp Ther* 2018.
- [69]. Stockstill K, Doyle TM, Yan X, Chen Z, Janes K, Little JW, Braden K, Lauro F, Giacotti LA, Harada CM, Yadav R, Xiao WH, Lionberger JM, Neumann WL, Bennett GJ, Weng HR, Spiegel S, Salvemini D. Dysregulation of sphingolipid metabolism contributes to bortezomib-induced neuropathic pain. *J Exp Med* 2018;215(5):1301–1313. [PubMed: 29703731]
- [70]. Storkson RV, Kjorsvik A, Tjolsen A, Hole K. Lumbar catheterization of the spinal subarachnoid space in the rat. *J Neurosci Methods* 1996;65(2):167–172. [PubMed: 8740594]
- [71]. Tham CS, Lin FF, Rao TS, Yu N, Webb M. Microglial activation state and lysophospholipid acid receptor expression. *Int J Dev Neurosci* 2003;21(8):431–443. [PubMed: 14659994]
- [72]. Treutwein B, Strasburger H. Fitting the psychometric function. *Percept Psychophys* 1999;61(1):87–106. [PubMed: 10070202]
- [73]. Volkow ND, McLellan AT. Opioid Abuse in Chronic Pain--Misconceptions and Mitigation Strategies. *The New England journal of medicine* 2016;374(13):1253–1263. [PubMed: 27028915]
- [74]. Walk RM, Elliott ST, Blanco FC, Snyder JA, Jacobi AM, Rose SD, Behlke MA, Salem AK, Vukmanovic S, Sandler AD. T-cell activation is enhanced by targeting IL-10 cytokine production in toll-like receptor-stimulated macrophages. *Immunotargets Ther* 2012;1:13–23. [PubMed: 27471682]
- [75]. Wang X, Loram LC, Ramos K, de Jesus AJ, Thomas J, Cheng K, Reddy A, Somogyi AA, Hutchinson MR, Watkins LR, Yin H. Morphine activates neuroinflammation in a manner parallel to endotoxin. *Proceedings of the National Academy of Sciences of the United States of America* 2012;109(16):6325–6330. [PubMed: 22474354]
- [76]. Watkins LR, Hutchinson MR, Rice KC, Maier SF. The “toll” of opioid-induced glial activation: improving the clinical efficacy of opioids by targeting glia. *Trends in pharmacological sciences* 2009;30(11):581–591. [PubMed: 19762094]
- [77]. Won JS, Singh I. Sphingolipid signaling and redox regulation. *Free radical biology & medicine* 2006;40(11):1875–1888. [PubMed: 16716889]

- [78]. Xie W, Strong JA, Kays J, Nicol GD, Zhang JM. Knockdown of the sphingosine-1-phosphate receptor S1PR1 reduces pain behaviors induced by local inflammation of the rat sensory ganglion. *Neuroscience letters* 2012;515(1):61–65. [PubMed: 22445889]
- [79]. Zhang Y, Chen K, Sloan SA, Bennett ML, Scholze AR, O’Keeffe S, Phatnani HP, Guarnieri P, Caneda C, Ruderisch N, Deng S, Liddelow SA, Zhang C, Daneman R, Maniatis T, Barres BA, Wu JQ. An RNA-sequencing transcriptome and splicing database of glia, neurons, and vascular cells of the cerebral cortex. *The Journal of neuroscience : the official journal of the Society for Neuroscience* 2014;34(36):11929–11947. [PubMed: 25186741]
- [80]. Zhu J, Liu Y, Pi Y, Jia L, Wang L, Huang Y. Systemic application of sphingosine 1-phosphate receptor 1 immunomodulator inhibits corneal allograft rejection in mice. *Acta Ophthalmol* 2014;92(1):e12–21. [PubMed: 23910624]

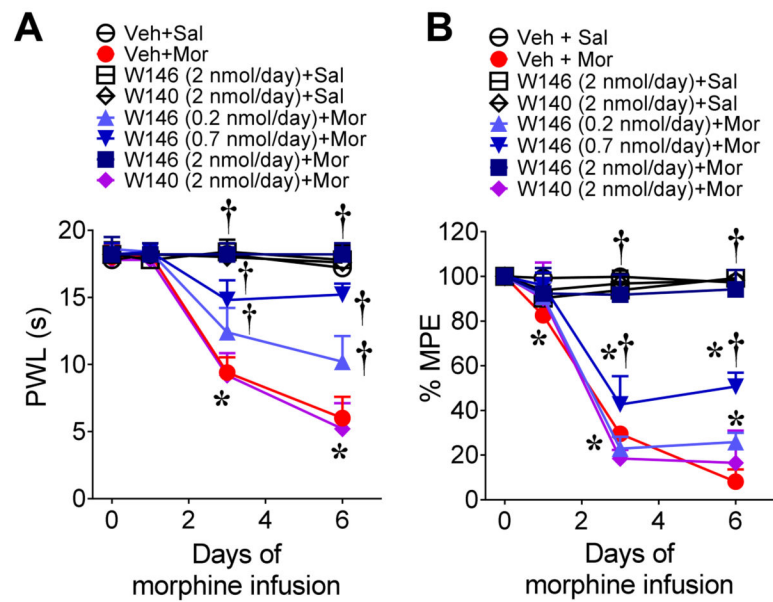


Fig. 1. Intrathecal delivery of W146 but not its inactive enantiomer, W140 prevents the development of OIH and antinociceptive tolerance.

(A,B) When compared to vehicle and saline-treated male rats, time-dependent hyperalgesia (A) and antinociceptive tolerance (B) developed in rats treated with morphine over 6 days.

Intrathecal administration of the S1PR1 antagonist W146, but not W140, blocked the development of OIH and tolerance in a dose-dependent manner. There were no effects on those rats treated with saline. [Time x treatment: (A) $F(21,96)=34$, $p=3.5 \times 10^{-35}$, $\eta^2_p=0.97$, $n=6$ /group; 48 animals with no exclusions; (B) $F(21,120)=59$, $p=2.5 \times 10^{-53}$, $\eta^2_p=0.98$, $n=5$ /group; 40 animals with no exclusions]. Results are mean \pm SD and analyzed by two-tailed, two-way ANOVA with Bonferroni comparisons. * $P<0.05$ vs. D0 and † $P<0.05$.

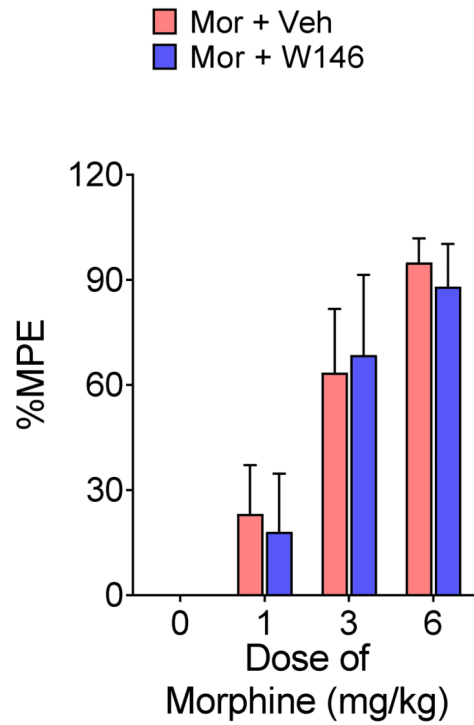


Fig. 2. S1PR1 inhibition does not alter acute morphine antinociceptive efficacy.

When measured at 30 min after acute morphine, the antinociceptive effects of morphine was not modified by W146 (2 nmol/day) or its vehicle in naïve male rats [Dose x Treatment: $F(3,24)=0.36$, $p=0.78$, $\eta^2_p=0.26$, $n=5$ /group; 10 animals with no exclusions]. Results are mean \pm SD and analyzed by two-tailed, two-way ANOVA with Bonferroni comparisons.

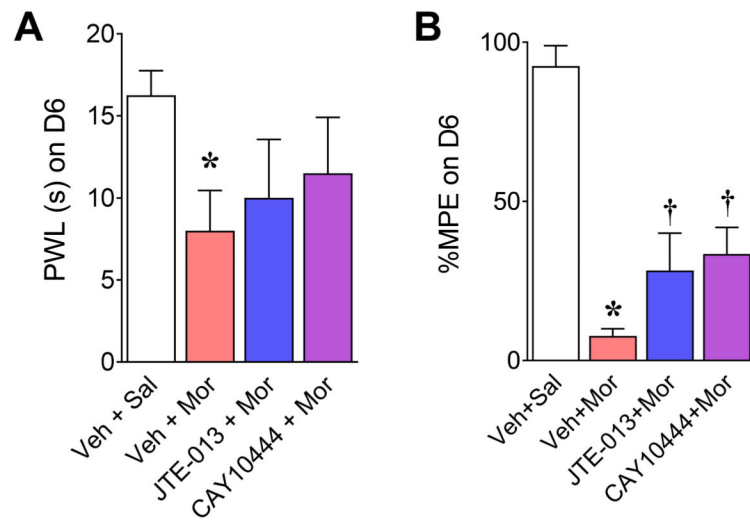


Fig. 3. Effects of S1PR2 and S1PR3 antagonists on OIH and antinociceptive tolerance. Intrathecal administration of a selective S1PR2 (JTE-013; 2 nmol/day) or S1PR3 (CAY10444; 2 nmol/day) antagonist in male rats had no significant effects on the development of hyperalgesia (**A**; $F(3,12)=6.1$, $p=0.0094$, $\eta^2=0.60$, $n=4/\text{group}$; 16 animals with no exclusions), but had modest, but significant, effects on tolerance (**B**; $F(3,12)=84$, $p=2.6 \times 10^{-8}$, $\eta^2=0.95$, $n=4/\text{group}$; 16 animals with no exclusions) in rats. Results are mean \pm SD and analyzed by two-tailed, one-way ANOVA with Dunnett's comparisons. * $P < 0.05$ vs. Veh+Sal; † $P < 0.05$ vs. Veh+Mor.

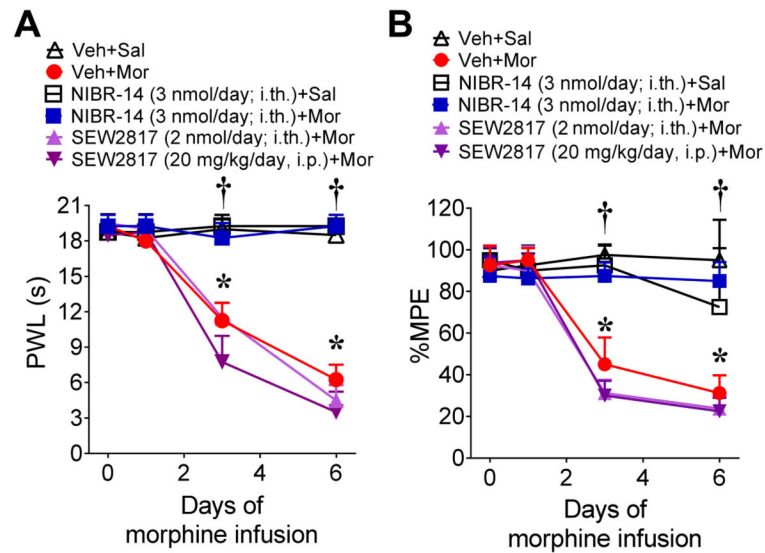


Fig. 4. S1PR1 antagonist, NIBR-14, but not the S1PR1 agonist, SEW2871, prevents the development of OIH and antinociceptive tolerance.

(A,B) When compared to vehicle and saline-treated male rats, time-dependent OIH (A) and antinociceptive tolerance (B) developed in rats treated with morphine over 6 days.

Intrathecal administration of the S1PR1 antagonist NIBR-14, but not the intrathecal or intraperitoneal administration of the S1PR1 agonist SEW2871, concurrent with morphine treatment over 6 days blocked the development of OIH and tolerance [Time x treatment: (A) $F(15,54)=44$, $p=1.1\times 10^{-24}$, $\eta^2_p=0.98$, $n=4$ /group, 24 animals with no exclusions; (B) $F(15,54)=11$, $p=1.5\times 10^{-11}$, $\eta^2_p=0.92$, $n=4$ /group; 24 animals with no exclusions]. Results are mean \pm SD and analyzed by two-tailed, two-way ANOVA with Bonferroni comparisons. * $P<0.05$ vs. D0 and † $P<0.05$.

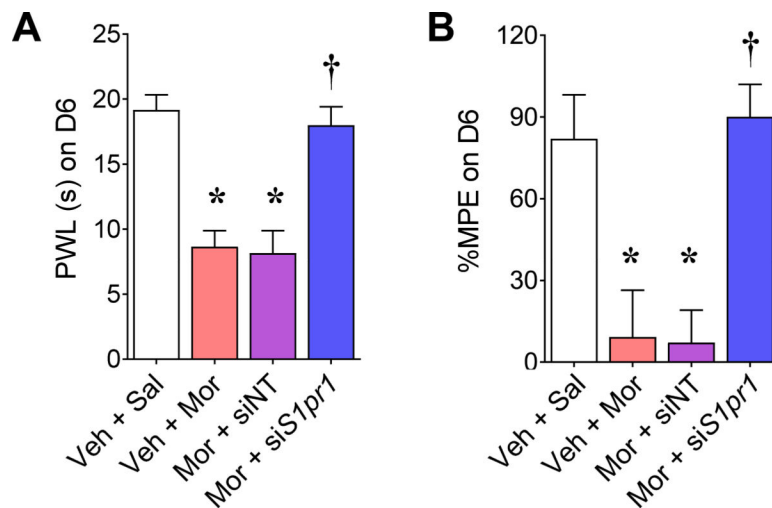


Fig. 5. Intrathecal delivery of *S1pr1*-targeting siRNA prevents the development of OIH and antinociceptive tolerance.

Intrathecal administration of *S1pr1*-targeting siRNA (siS1PR1; 2 μ g on days 1, 2 and 4) has been shown to reduce S1PR1 expression in the spinal cord by at least 45% [69]. Intrathecal administration of siS1PR1 in male rats, but not a non-targeting siRNA (siNT), blocked the development of hyperalgesia (**A**; $F(3,20)=107$, $p=1.8\times 10^{-12}$, $\eta^2=0.94$, $n=6/\text{group}$, 24 animals with no exclusions) and tolerance (**B**; $F(3,20)=58$, $p=58$, $\eta^2=0.90$, $n=6/\text{group}$, 24 animals with no exclusions). Results are mean \pm SD and analyzed by two-tailed, one-way ANOVA with Dunnett's comparisons. * $P<0.05$ vs. Veh+Sal and † $P<0.05$ vs. Veh+Mor.

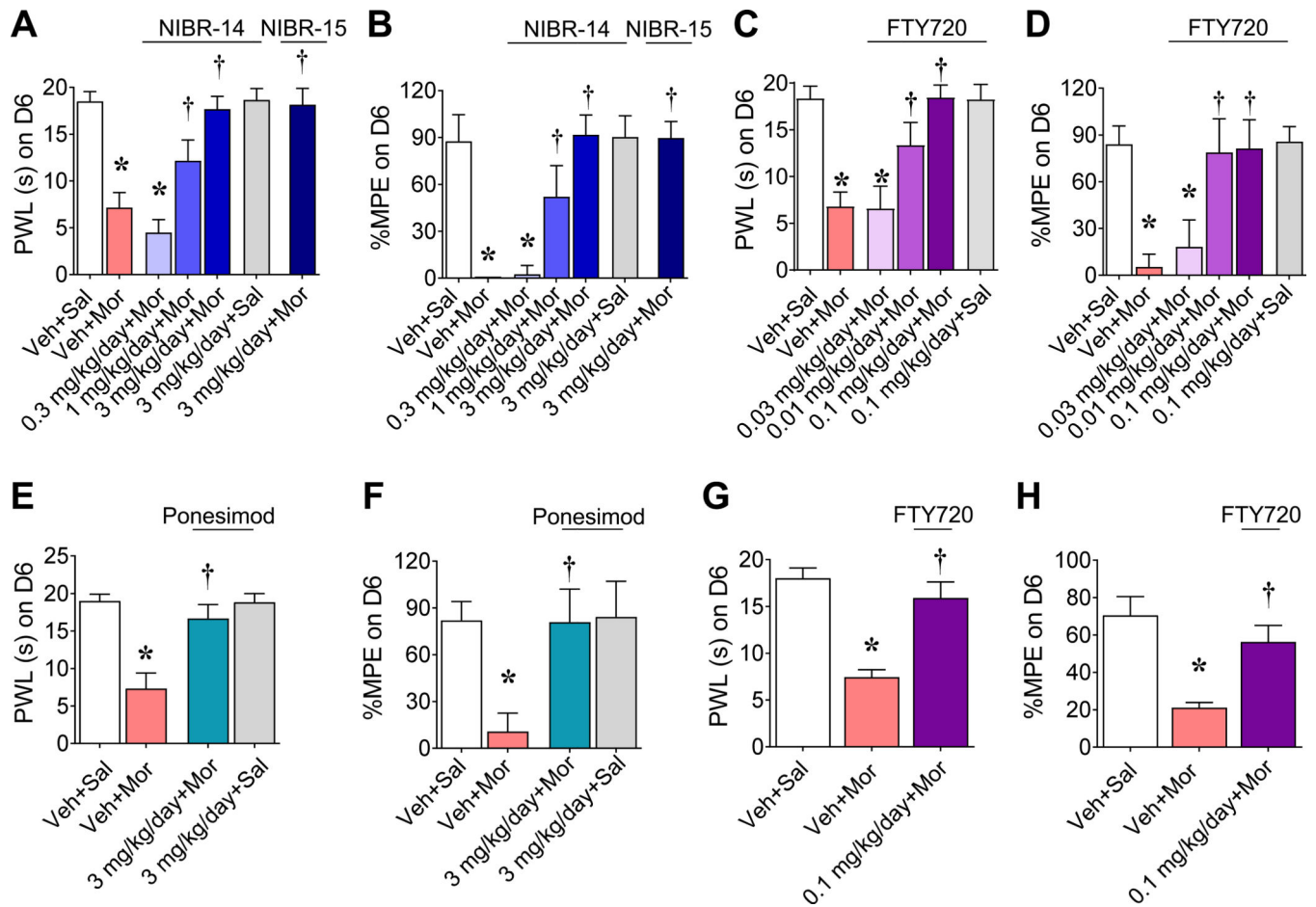


Fig. 6. Oral administration of functional and competitive S1PR1 antagonists prevents the development of OIH and antinociceptive tolerance.

In male rats, the development of thermal hyperalgesia and antinociceptive tolerance by day six was blocked by oral administration of NIBR-14 or NIBR-15 (**A, B**), FTY720 (**C, D**; $n=9$ /group) or ponesimod (**E, F**). (**G, H**) In female rats, oral administration of FTY720 (0.1 mg/kg/day) also blocked the development of thermal hyperalgesia and antinociceptive tolerance by day 6. Results are mean \pm SD and analyzed by two-tailed, one-way ANOVA with Dunnett's comparisons. [Treatment: (**A**) $F(5,30)=99$, $p=1.0\times 10^{-17}$, $\eta^2=0.94$, $n=6$ /group, 42 animals with no exclusions; (**B**) $F(5,24)=52.9$, $p=3.5\times 10^{-12}$, $\eta^2=0.92$, $n=5$ /group, 40 animals with no exclusions; (**C**) $F(5,48)=86.4$, $p=8.3\times 10^{-23}$, $\eta^2=0.90$, $n=9$ /group, 54 animals with no exclusions; (**D**) $F(5,48)=52.2$, $p=2.9\times 10^{-18}$, $\eta^2=0.84$, $n=9$ /group, 24 animals with no exclusions; (**E**) $F(3,20)=73.9$, $p=5.4\times 10^{-11}$, $\eta^2=0.92$, $n=6$ /group, 48 animals with no exclusions and (**F**) $F(3,16)=20.6$, $p=9.6\times 10^{-6}$, $\eta^2=0.79$, $n=5$ /group, 24 animals with no exclusions; (**G**) $F(2,17)=120$, $p=6.0\times 10^{-10}$, $\eta^2=0.94$, $n=6$ /group, 18 animals with no exclusions and (**H**) $F(2,17)=63$, $p=5.1\times 10^{-8}$, $\eta^2=0.89$, $n=6$ /group, 18 animals with no exclusions] * $P<0.05$ vs. Veh+Sal and † $P<0.05$ vs. Veh+Mor.

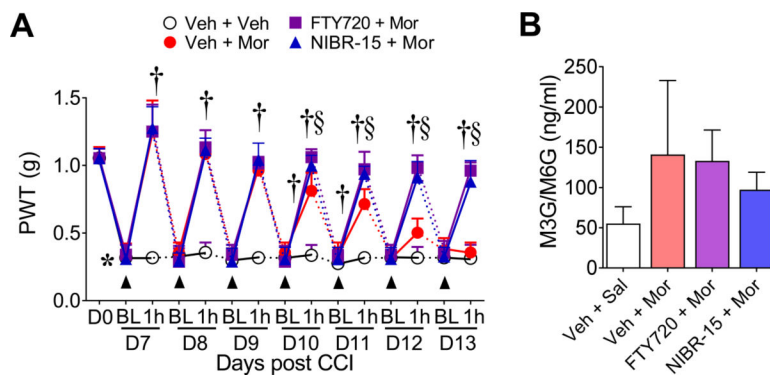


Fig. 7. Oral administration of S1PR1 antagonists prevents the development of anti-allodynic tolerance in mice with traumatic nerve injury.

(A) By day 7 post CCI-surgery, mechano-allodynia in male mice was evoked by von Frey filaments applied to the paw ipsilateral to CCI. When compared to the vehicle + saline group ($n=4$) on day 7, mice receiving subcutaneous injections of morphine with vehicle ($n=4$) had attenuated mechano-allodynia. The anti-allodynic effect of morphine was lost during repeated daily administration (anti-allodynic tolerance). Oral administration of FTY720 (0.03 mg/kg/day; $n=5$) and NIBR-15 (0.3 mg/kg/day; $n=5$) with daily morphine injection blocked the development of morphine-induced anti-allodynic tolerance. [Time x treatment: $F(18,98)=10.4$, $p=1.1 \times 10^{-15}$, $\eta^2_p=0.91$, 18 animals with no exclusions]. (B) When measured on day 13, the plasma levels of morphine metabolites (M3G/M6G) were not altered amongst the groups [Treatment: $F(3,14)=2.6$, $p=0.093$, $\eta^2=0.36$, 18 animals with no exclusions]. Results are mean \pm SD and analyzed by two-tailed, (A) two-way ANOVA with Bonferroni comparisons or (B) one-way ANOVA with Dunnett's comparisons. * $P < 0.05$ vs. day (D)0; † $P < 0.05$ vs D7; § $P < 0.05$ vs. Veh+Mor.

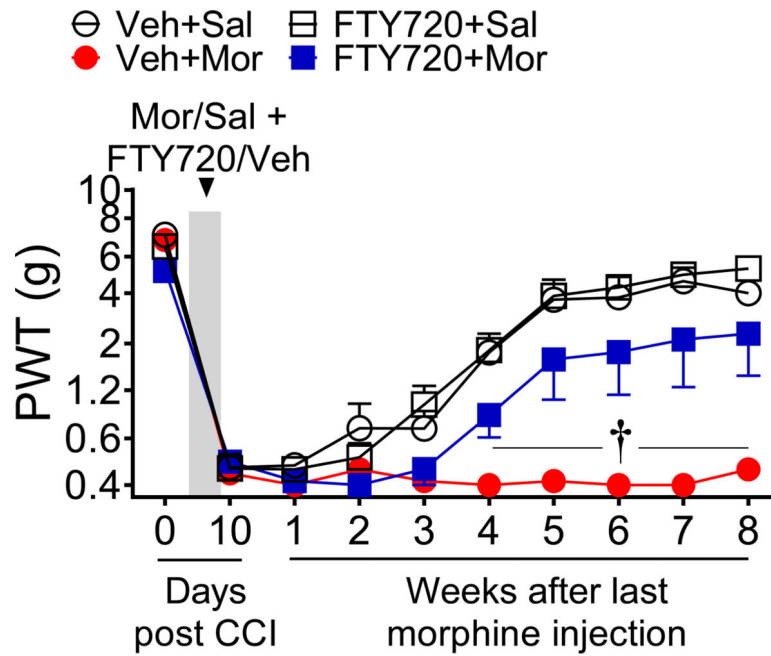


Fig. 8. Oral administration of S1PR1 antagonists attenuates morphine-induced persistence of neuropathic pain.

Neuropathic pain induced by CCI in male F344 rats treated with saline for 5 days resolved itself by 7–8 weeks post-CCI. In contrast, morphine treatment extended the persistence of neuropathic pain through 8 weeks post-CCI. The interval of morphine-induced persistent sensitization was significantly reduced with intraperitoneal administration of a low dose of FTY720 (0.1 mg/kg/day) during morphine treatment. FTY720 had no effect in saline-treated animals. [Time x treatment: $F(27,200)=5.7$, $p=1.0\times 10^{-13}$, $\eta^2_p=0.85$, $n=6/\text{group}$, 24 animals with no exclusions]. Results are mean \pm SEM and analyzed by two-tailed, two-way ANOVA with Bonferroni comparisons. † $P<0.05$ vs. Veh+Mor.

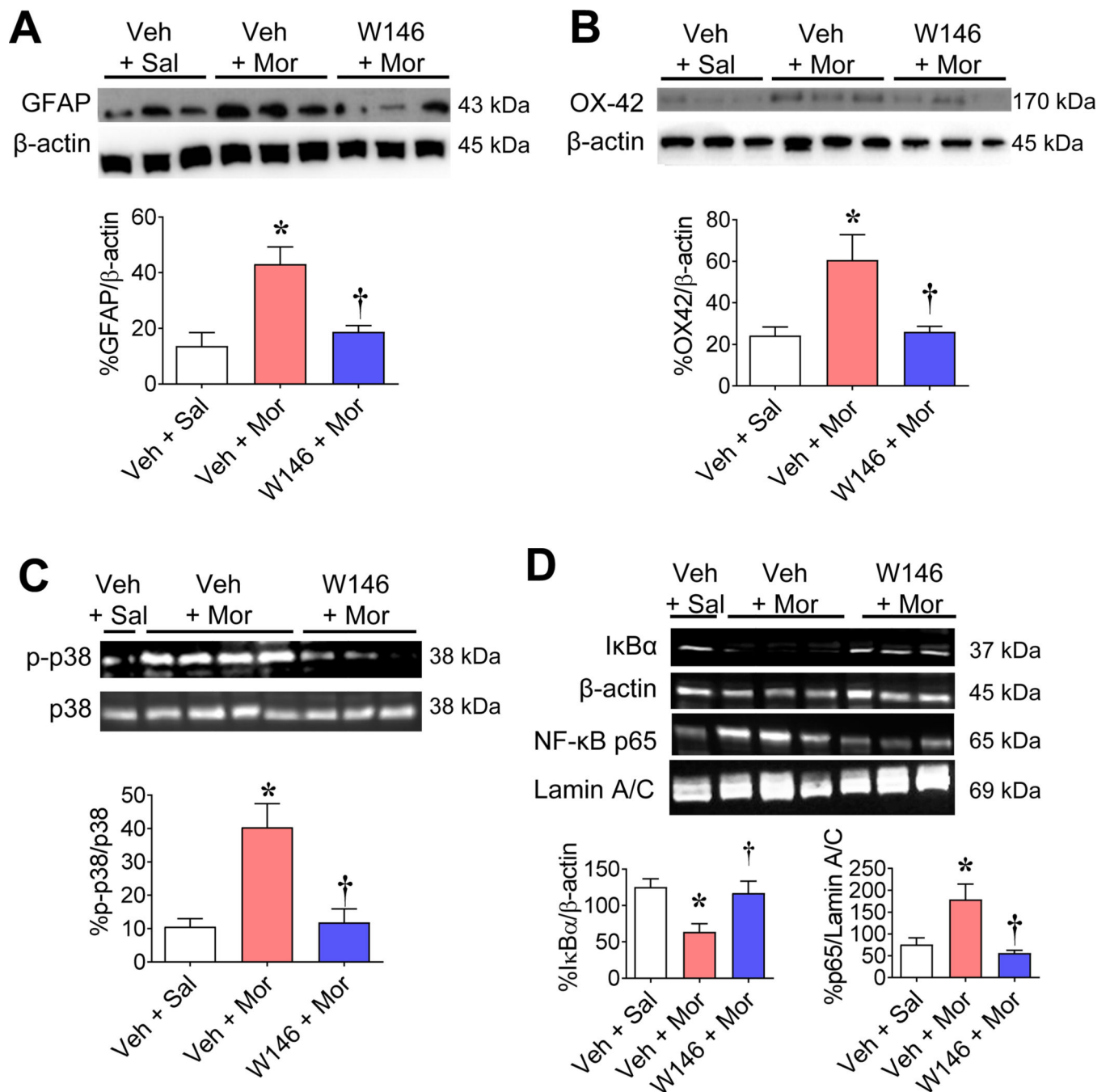


Fig. 9. Intrathecal administration of W146 blocks the development of morphine-induced neuroinflammation in the dorsal horn of the spinal.

When compared on day 6 to rats treated with vehicle and saline, the expression of GFAP (astrocytes; **A**) and OX-42 (microglia; **B**) increased in the dorsal horns of the spinal cord from male rats treated with morphine infusion. Intrathecal injection of W146 (2 nmol/day; **A,B**) blocked morphine-induced GFAP and OX-42 expression. (**C,D**) When compared to Veh + Sal treated rats on day six, phosphorylation p38 increased (**C**), cytosolic I κ B α decreased (**D**) and nuclear translocation of NF κ B p65 increased (**D**) in the dorsal horn of the spinal cord from rats treated with morphine. These events were blocked with intrathecal

injections of W146 (2 nmol/day; **C,D**). Using ImageJ [66], the images for β -actin (**A, B**) were inverted from the original blot image. All blots were cropped for clarity. Results are expressed as mean \pm SD for n=6 rats/group (54 animals with no exclusions) and analyzed by two-tailed, one-way ANOVA with Dunnett's comparisons. [Treatment: (**A**) GFAP: F(2,15)=67, $p=3.4\times 10^{-8}$, $\eta^2=0.90$; (**B**) OX-42: F(2,15)=44, $p=5.0\times 10^{-7}$, $\eta^2=0.86$; (**C**) F(2,15)=71, $p=2.2\times 10^{-18}$, $\eta^2=0.90$; (**D**) I κ B α : F(2,15)=39, $p=1.2\times 10^{-6}$, $\eta^2=0.84$; NF κ B p65: F(2,15)=52, $p=1.8\times 10^{-7}$, $\eta^2=0.87$. *P<0.05 vs. Veh+Sal and †P<0.05 vs. Veh+Mor.

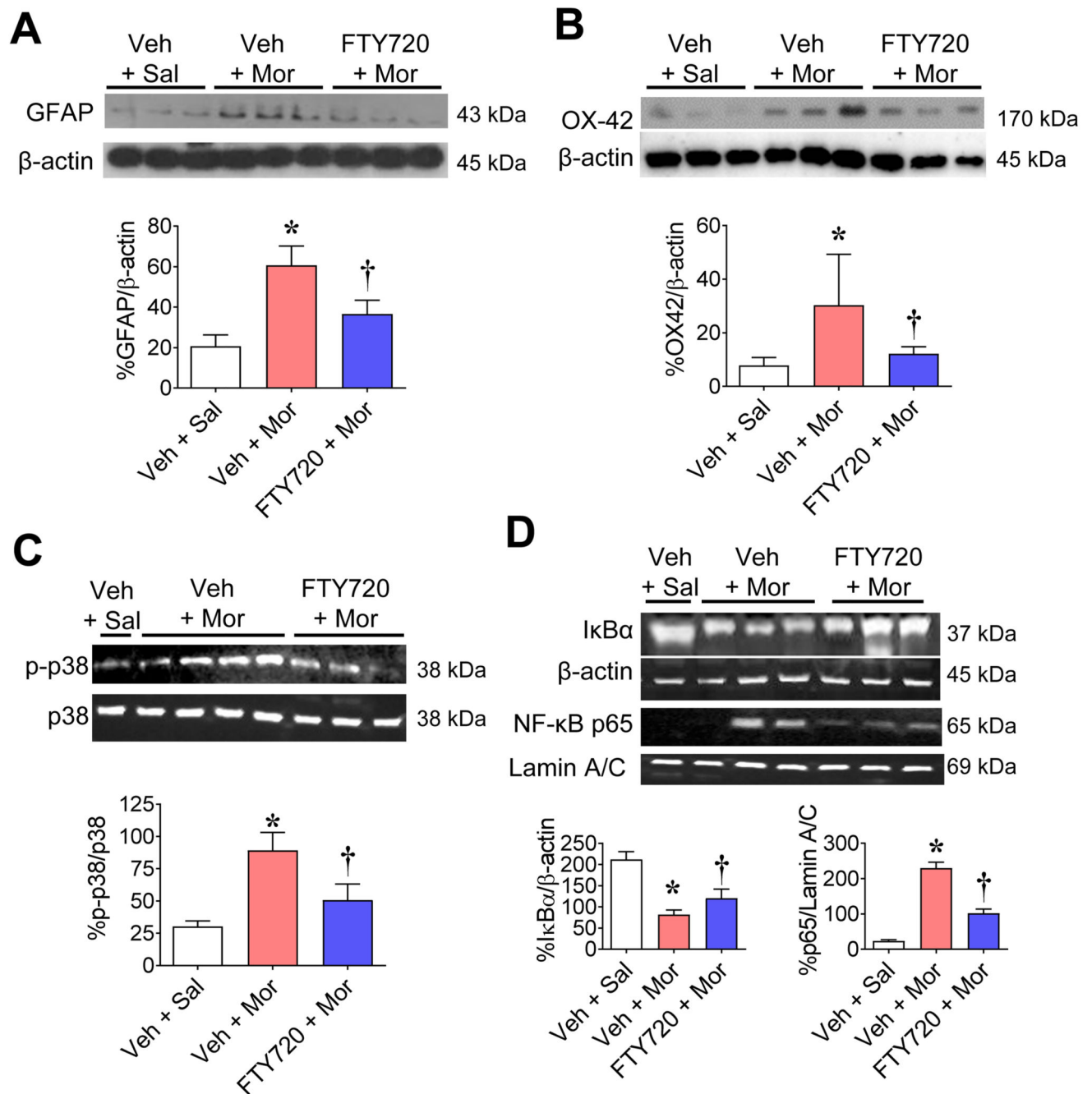


Fig. 10. Oral administration of FTY720 blocked morphine-induced neuroinflammation in the dorsal horn of the spinal cord.

(A,B) When compared on day 6 to rats treated with vehicle and saline, the expression of GFAP (astrocytes; A) and OX-42 (microglia; B) increased in the dorsal horns of the spinal cord from male rats treated with morphine infusion. Oral administration of FTY720 (0.1 mg/kg/day) blocked morphine-induced GFAP and OX-42 expression. (C,D) When compared to Veh + Sal treated rats on day six, phosphorylation p38 increased (C), cytosolic I κ B α decreased (D) and nuclear translocation of NF κ B p65 increased (D) in the dorsal horn

of the spinal cord from rats treated with morphine. These events were blocked with oral administration of FTY720 (0.1 mg/kg/day; **C,D**). Using ImageJ [66], the images for β -actin (**B**) were inverted from the original image and the brightness and contrast was adjusted across the blots for **D**: NF κ B p65. All blots were cropped for clarity. Results are expressed as mean \pm SD for n=6 rats/group (54 animals with no exclusions) and analyzed by two-tailed, one-way ANOVA with Dunnett's comparisons. [Treatment: (**A**) GFAP: F(2,15)=43, $p=5.8\times 10^{-7}$, $\eta^2=0.85$; (**B**) OX-42: F(2,15)=6.9, $p=0.0076$, $\eta^2=0.48$; (**C**) p-p38: F(2,15)=45, $p=4.9\times 10^{-7}$, $\eta^2=0.86$; (**D**) I κ B α : F(2,15)=377, $p=1.5\times 10^{-13}$, $\eta^2=0.98$; NF κ B p65: F(2,15)=474, $p=2.8\times 10^{-14}$, $\eta^2=0.98$. * $P<0.05$ vs. Veh+Sal and † $P<0.05$ vs. Veh+Mor.

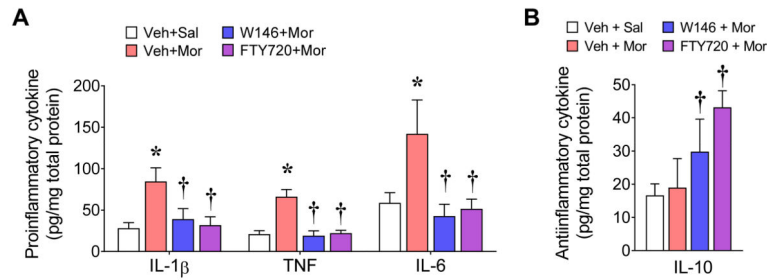


Fig. 11. Oral administration of functional and competitive S1PR1 antagonists block morphine-induced neuroinflammatory cytokine production in the dorsal horn of the spinal cord.

(A) When compared on day 6 to rats treated with vehicle and saline, IL-1 β , TNF and IL-6 expression increased in the dorsal horn of the spinal cord from male rats treated with morphine, which was blocked in rats that received intrathecal injections of W146 (2 nmol/day) or oral administrations of FTY720 (0.1 mg/kg/day). (B) In contrast, the levels of the anti-inflammatory/neuro-protective cytokine IL-10 increased in the dorsal horn of the spinal cord in mice treated with intrathecal W146 (2 nmol/day) or oral FTY720 (0.1 mg/kg/day) during morphine treatment. Morphine alone did not significantly alter IL-10 expression. Results are expressed as mean \pm SD for n=6 rats/group (24 animals with no exclusions) and analyzed by two-tailed, one-way ANOVA with Dunnett's comparisons. [Treatment: (A) IL-1 β : F(3,20)=29, $p=1.9\times 10^{-7}$, $\eta^2=0.81$; TNF: F(3,20)=90, $p=9.2\times 10^{-12}$, $\eta^2=0.93$, IL-6: F(3,16)=20, $p=1.3\times 10^{-5}$, $\eta^2=0.79$; and (B) F(3,20)=17, $p=1.1\times 10^{-5}$, $\eta^2=0.72$]. *P<0.05 vs. Veh+Sal and †P<0.05 vs. Veh+Mor.